Mon. Not. R. Astron. Soc. **000**, 000–000 (0000) Printed 5 February 2008 (MN LATEX style file v2.2)

Five WC9 stars discovered in the AAO/UKST Hα survey

E. C. Hopewell[1], M. J. Barlow[2], J. E. Drew[1], Y. C. Unruh[1], Q. A. Parker[3,4], M. J. Pierce[5], P.A.Crowther[6], C. Knigge[7], S. Phillipps[5], A. A. Zijlstra[8]

[1]*Imperial College of Science, Technology and Medicine, Blackett Laboratory, Exhibition Road, London, SW7 2AZ, U.K.*
[2]*University College London, Department of Physics & Astronomy, Gower Street, London WC1E 6BT, U.K.*
[3]*Department of Physics, Macquarie University, NSW 2109, Australia*
[4]*Anglo-Australian Observatory, PO Box 296, Epping NSW 1710, Australia*
[5]*Astrophysics Group, Department of Physics, Bristol University, Tyndall Avenue, Bristol, BS8 1TL, U.K.*
[6]*Department of Physics & Astronomy, University of Sheffield, Hicks Building, Hounsfield Rd, Sheffield, S3 7RH, U.K.*
[7]*Department of Physics and Astronomy, University of Southampton, Southampton SO17 1BJ, UK.*
[8]*The University of Manchester, School of Physics & Astronomy, PO Box 88, Manchester M60 1QD, U.K.*

5 February 2008

ABSTRACT

We report the discovery of 5 massive Wolf-Rayet (WR) stars resulting from a programme of follow-up spectroscopy of candidate emission line stars in the AAO/UKST Southern Galactic Plane Hα survey. The 6195-6775 Å spectra of the stars are presented and discussed. A WC9 class is assigned to all 5 stars through comparison of their spectra with those of known late-type WC stars, bringing the known total number of Galactic WC9 stars to 44. Whilst three of the five WC9 stars exhibit near infrared (NIR) excesses characteristic of hot dust emission – as seen in the great majority of known WC9 stars – we find that two of the stars show no discernible evidence of such excesses. This increases the number of known WC9 stars without NIR excesses to 7. Reddenings and distances for all 5 stars are estimated.

Key words: stars: Wolf-Rayet – stars: circumstellar matter – Galaxy: stellar content – surveys

1 INTRODUCTION

Massive Wolf-Rayet stars are important objects of study for two reasons. First, the Wolf-Rayet (WR) phase of massive star evolution has itself been a significant challenge to models of extreme mass loss (Hillier 2003) and represents the likely precursor stage to chemically-peculiar core-collapse supernovae (type Ib and Ic: Woosley, Heger & Weaver, 2002), which has directed attention toward understanding their structure and variety. Second, their galactic demographics both as a function of WR sub-type and, more generally, as markers of star-forming activity has also attracted attention in order to achieve a better understanding of their stellar evolutionary origins (Maeder & Meynet 2000) and their impact, as luminous objects blowing chemically-enriched, high-speed winds into their galactic environments (e.g. Homeier et al 2003).

WR stars possess very distinctive spectra, dominated by high-contrast, broad emission lines. This reflects the strong mass loss that follows on from the loss of the hydrogen-rich atmosphere that these stars were born with, as higher mass ($\gtrsim$ 25 M$_\odot$) O stars. WR stars are most commonly H-deficient objects, and so do not normally display prominent hydrogen emission lines in their spectra, but are characterised instead by strong emission lines of He, N and C. The equivalent width ratios between the various emission lines in WR spectra allow their classification into subclasses and subtypes. WR stars whose spectra are dominated by lines of nitrogen and helium are termed WN stars, whilst stars displaying strong carbon, oxygen and helium lines are assigned WC or WO classifications. Subtypes then refer to the ionisation degree of the star with the WN 3–9 and WC 4–9 sequences each going from higher to lower ionisation states.

This paper presents the discovery of five Galactic massive Wolf-Rayet stars, by means of spectroscopic follow-up of the Anglo-Australian Observatory United Kingdom Schmidt Telescope (AAO/UKST) Hα Survey of the Southern Galactic Plane and Magellanic Clouds (Parker et al 2005). These new discoveries are located in a relatively small sky area, roughly centred on $\ell \sim 339^{\rm o}, b \sim 1^{\rm o}$ and spanning just 4×2 square degrees. The exceptionally dense young star cluster Westerlund 1 (Westerlund 1987, Clark & Negueruela 2002) lies near the edge of this region. Intriguingly, these 5 objects were the only WR stars discovered in spectroscopy of targets within a larger 62 square degree area, which also yielded more than 70 new Hα emission line stars (Hopewell et al, in prep). Two of our discoveries lie within the sky area covered by Shara et al (1991, 1999), in their blue narrowband search for WR stars.

It is striking that all five new WR stars are shown to belong to the same spectral sub-type – WC9 – and all are reasonably bright, with R magnitudes in the range $14 \lesssim R \lesssim 16$. The total number of known galactic WC9 stars previously stood at 39 (van der Hucht 2001: 30, Homeier et al. 2003: 3, LaVine, Eikenberry &

Davis 2003: 2, Negueruela & Clark 2005: 4 in Wd 1)) and as such the five discoveries reported here represent a significant addition to this sample. The observations revealing them were obtained a year after and using the same spectroscopic facility as the discovery observations of only the fourth known Galactic WO star, WR 93b (Drew et al. 2004).

The AAO/UKST Hα Survey of the Southern Galactic Plane and Magellanic Clouds was the last photographic UKST sky survey to be carried out. It is described in full by Parker et al (2005). It was a narrow band photographic sky survey of the entire Southern plane of the Milky Way for galactic latitudes $-10^{\circ}<$ b $<$ + 10 $^{\circ}$ and consisted of 233 Galactic Plane and 40 Magellanic Cloud fields on 4-degree centres. The survey was completed in 2003 and is available online, as SuperCOSMOS scans of the original survey films at 10 μm resolution (SHS database, located at http://www-wfau.roe.ac.uk/sss/halpha/). This survey used a high specification, single element Hα interference filter with a 70 Å bandpass. This, together with fine-grained Tech-Pan emulsion as the detector, allowed a survey of Galactic ionised hydrogen, combining large area coverage with good sensitivity and arcsecond resolution. For each field the aim was to take 15-minute broad-band short-red exposures alongside the 3-hour Hα exposures to produce contemporaneous exposure pairs. In the SHS, the Hα and short-red data are combined with *I* band data from the older UKST IVN Southern Sky Survey.

Since the completion of the survey, a programme of spectroscopic confirmation of point-source candidate Hα emitters from the SHS database has been undertaken, using the UKST 6dF multi-object facility. This programme is finding all types of Hα emitting point sources in the Galaxy, many of which represent short-lived evolutionary phases which are, correspondingly, rarely observed. Here the focus is on WR stars: their detection via the UKST survey and SHS database, typically resulting from the inclusion of the strong He II and/or C II lines at $\sim$ 6570 Å within the Hα filter bandpass.

The paper is organised as follows. The next section discusses the method of target selection used for the UKST 6dF follow-up spectroscopy program and gives magnitudes and positions for the new WR stars. Section 3 then provides information about the observations and explains the relevant data reduction procedures. The 6dF data, details of spectral subtype identification and comments on individual spectra are presented in Section 4. We then consider estimates of the dust emission, reddening and distances to the new WR stars in Section 5. Finally, we close in Section 6 with a comparison of this red selection of WR stars to selections made at other wavelengths, and a brief comment on how these new stars relate to the previously known WC9 sample.

2 SELECTION OF SPECTROSCOPIC TARGETS FROM THE UKST Hα SOUTHERN GALACTIC PLANE SURVEY

The discovery of the five new WC9 stars presented in this paper resulted from observations of SHS fields HAL0348, HAL0349, HAL0413 and HAL0414, whose field centers and positions are shown in Table 1. As would be expected for fields straddling the galactic equator, HAL0349 and HAL0414 are highly reddened regions with *E(B–V)*$>$ 3 predicted for extragalactic objects observed along these sightlines (Schlegel, Finkbeiner & Davis 1998). These fields also include a few extremely reddened regions for which *E(B–V)*$\gtrsim$ 15. Fields HA0348 and HAL0413 lie a few degrees higher in galactic latitude, and consequently cover regions of less intense reddening where the average extinctions are $1 \lesssim$ *E(B–V)*$\lesssim 2.5$ and $1 \lesssim$ *E(B–V)*$\lesssim 6$ respectively.

Table 1. $4^{\circ} \times 4^{\circ}$ AAO/UKST Hα Survey field centers in 1950 and Galactic co-ordinates.

Field	RA (1950)	Dec (1950)	ℓ	b
HAL0348	16 00 00	-48 00 00	332.7	$+3.3$
HAL0349	16 24 00	-48 00 00	335.7	$+0.5$
HAL0413	16 30 00	-44 00 00	339.3	$+2.5$
HAL0414	16 52 00	-44 00 00	341.9	-0.4

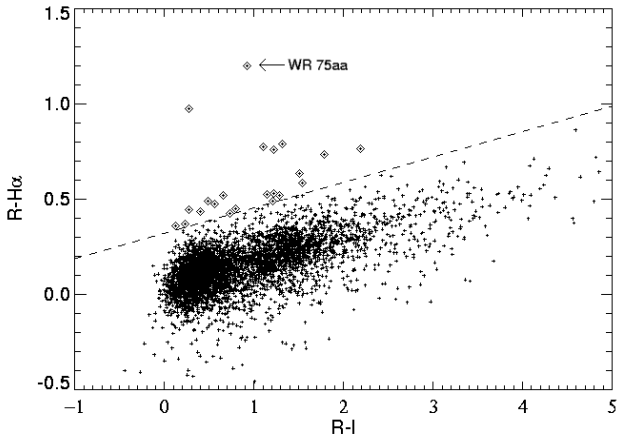

Figure 1. A plot of (R-Hα) versus (R-I) for all SHS catalogue point sources within the 1° box containing WR 75aa which satisfy $14 < R < 16.3$ as given by the SHS database. The dashed line indicates the selection limit whilst the diamonds show the sources that were selected for spectroscopic follow-up

When selecting this region of the galactic plane for follow-up we were motivated in part by the presence of the star cluster Westerlund 1 in the corner of HAL0414. Westerlund 1 is a highly reddened young open cluster whose population has been shown to be rich in massive post-main-sequence stars (Westerlund 1987; Clark & Negueruela 2002; Clark et al. 2005). These studies have revealed a considerable population of supergiants, hypergiants and Wolf-Rayet stars in the cluster and prompted us to observe the surrounding region to investigate the environment of this extraordinary cluster.

Target selection was conducted by considering the positions of the objects in a plot of $(R-I)$ colour versus $(R-H\alpha)$ excess for all SHS point sources within a specified R magnitude range. However within these $4^{\circ} \times 4^{\circ}$ fields the location of the stellar locus in this colour-colour plot can be seen to change with position in the field, owing to variations in the effective magnitude calibration across it. Therefore, when identifying the objects for spectroscopic follow-up, the fields were broken down into 16 smaller $1^{\circ} \times 1^{\circ}$ regions and the Hα emission candidates selected from these subsamples. Two magnitude ranges were considered separately for selecting targets, $12 < R < 14.5$ and $14.5 < R < 16.3$. Figure 1 demonstrates how the targets were selected for the area that contained WR 75aa, one of the new discoveries. From this sample of $\sim$ 5000 stars, 22 were selected as candidates for follow-up spectroscopy, all falling between $0 < (R-I) < 3$ and on the Hα ex-

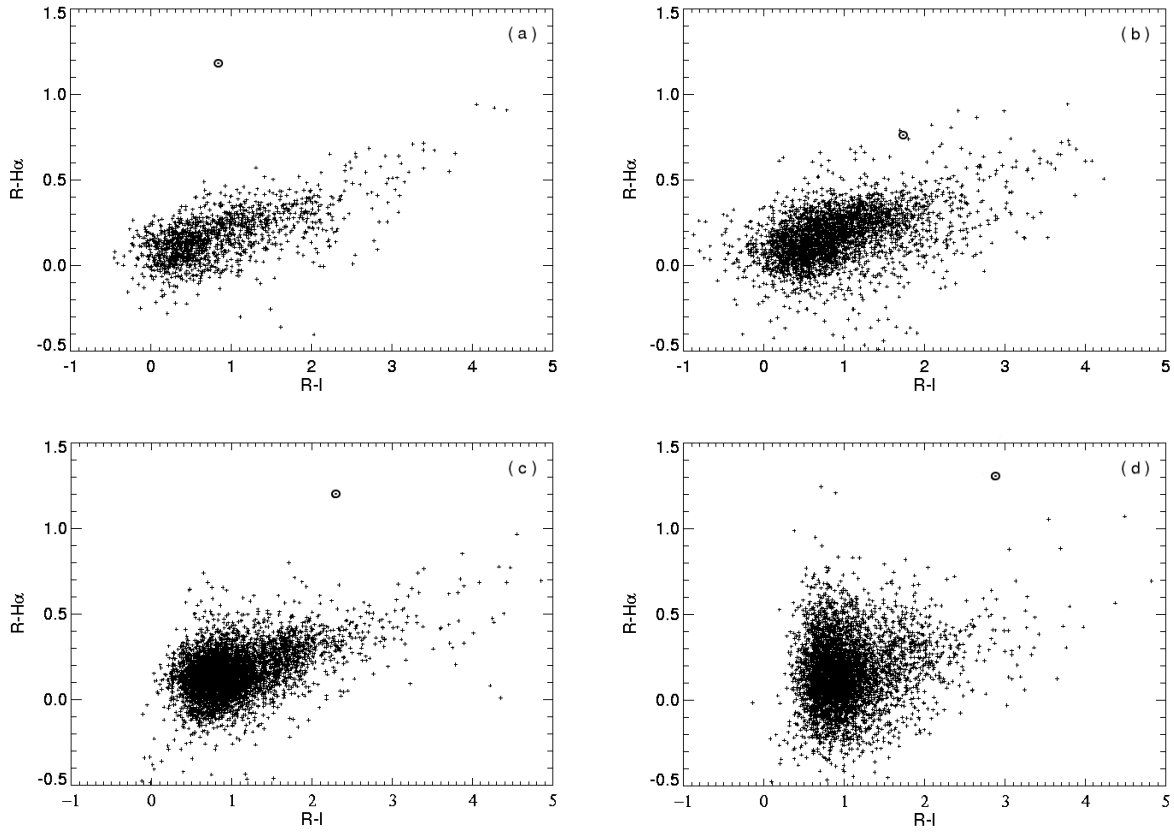

Figure 2. (R-I) versus (R-Hα) for the $1^{o} \times 1^{o}$ boxes containing (a) WR 75c; (b) WR 75d; (c) WR 77aa; and (d) WR 77t. The WR stars are highlighted by open circles.

Table 2. Designations (including J2000 positions) and SHS magnitudes for the new Wolf-Rayet stars. The WR catalogue names in the left-hand column are named according to the conventions of the van der Hucht (2001) catalogue of massive WR stars.

WR No	SHS designation	SHS Field	ℓ	b	SuperCOSMOS Magnitudes Hα	R	I
75aa	SHS J162620.2-455946	413	337.02	+2.17	13.85	15.31	14.18
75c	SHS J163403.6-434025	413	339.65	+2.77	12.78	13.96	13.12
75d	SHS J163417.5-460852	349	337.86	+1.06	13.27	14.03	12.30
77aa	SHS J164646.3-454758	414	339.56	−0.33	14.59	15.79	13.51
77t	SHS J165057.6-434028	414	341.66	+0.47	14.57	15.87	13.00

cess side of the main stellar locus. Objects with $(R - H\alpha)$ colours in the excess region, but $(R - I) > 3$, were not selected as this region of the plot becomes increasingly populated with late type stars, whose optical spectra contain molecular bands, which lead to their colours mimicking those of Hα excess objects. WR stars require $\sim$ *E(B–V)* > 5 in order to display such colours, so this selection cut also serves to exclude severely reddened stars.

Basic data for the five new Wolf-Rayet stars, including the initial SuperCOSMOS magnitudes used to select these objects as targets, are given in Table 2. The R and Hα magnitudes in the table refer to the AAO/UKST measurements, however the I magnitudes listed in the SHS catalogue were derived through matching SHS sources with I band data from UKST IVN Surveys. WR star names have been assigned in line with the convention used within the seventh catalogue of Wolf-Rayet stars (van der Hucht, 2001) and we will hereafter refer to the new WR stars by these designations.In Table 2, we also introduce the IAU-registered naming convention for stars picked out from the SHS: namely, SHS JHHMMSS.s+DDMMSS (J2000 coordinates).

From figures 1 and 2 it can be seen that, with the possible exception of WR 75d, the new WC9 stars were obvious high priority candidates for spectroscopic follow-up, displaying the largest $(R-\mathrm{H}\alpha)$ excesses in their subfields. WR 75d appears to lie in a more populated region of the diagram. However the objects nearby were nearly all discounted for follow-up as on closer inspection they were revealed to have spurious Hα excesses resulting from the confusion of two or more objects in the digitising process.

In the case of the candidate which became WR 75aa, the process of checking selected targets against known objects revealed that it had already been identified as a possible Hα emission line star. Known as SPH 146, it was detected in the southern objective prism survey for Hα emission objects published by Schwartz, Pers-

son & Hamann (1977): they described it as showing faint/uncertain Hα emission.

3 UKST/6DF OBSERVATIONS

Spectroscopic follow-up observations of eight SHS fields were obtained using the AAO/UK Schmidt 6dF multi-fibre spectrograph on 26–30 March 2004, three of which (HA0349, HA0413 and HA0414) contained the new WR stars presented here. Details of the observations can be found in Table 3. Observations were made using the 1516R grating, which in conjunction with a 1024×1024 EEV detector having 13μm pixels yields a spectral resolution of $\sim$ 2 Å and a spectral range of 6195-6775 Å. For the spectra presented in this paper the observations involved taking both on-target and sky-offset frames to allow for varying levels of diffuse Hα emission in the vicinity of our targets.

The data were extracted from the CCD frames and reduced using 6dfdr, the 6dF adaption of the 2dfdr software package (see http://www.aao.gov.au/AAO/2df/manual.htm). Each object and sky-offset frame was reduced separately before being combined and then subtracted to produce the final spectra. For every frame, this reduction involved: flat field extraction; fibre-by-fibre arc extraction and calibration; extraction of the observed spectrum from each fibre with scattered light correction. Each frame was also processed for cosmic ray hits, which the software removed by assuming that these corresponded to $>20\sigma$ outliers. No fibre throughput calibration was applied to these data. Once the individual frames were reduced, the sky offset frames were reexamined to identify any fibres including unwanted starlight and, if possible, to replace them with uncontaminated data from a different skyframe. No replacement was necessary for any of the offset pointings associated with the new Wolf-Rayet stars. The reduced frames were then processed in 6dfdr to produce two combined averaged frames, one for the object frames and another for the sky offsets. The sky subtraction was then accomplished using FIGARO routines within the Starlink software suite to subtract the combined offset frame from the combined object frame, after appropriate scaling. This reduction process yielded a single wavelength-calibrated frame for each field which contained between 80 and 120 spectra, each of 1032 pixels. As a final measure prior to analysis, the spectra for WR 77aa and WR 77t – the faintest of this sample – were redistributed into 2 pixel bins to reduce the noise level.

4 THE 6DF SPECTRA OF THE 5 WR STARS

The extracted stellar spectra are shown in figure 3. It is immediately evident that all five stars are of a similar spectral subtype. The emission lines present have been identified through use of the Atomic Line List v 2.04 maintained by P. van Hoof,(http://www.pa.uky.edu/$\sim$peter/atomic/), and are listed in Table 4. All are due to ionised species of helium and carbon.

Initial identification of the spectral subtype of these stars was accomplished though comparison of the 6dF spectra with the spectrophotometry of Wolf-Rayet stars presented by Torres-Dodgen & Massey (1988). This allowed all five to be identified as belonging to the WC9 subtype. Figure 4, illustrates the trends present among late type WC stars and confirms our assignments as we now describe.

The spectra shown in figure 4 illustrate the fact that as the WR subtype decreases toward earlier types of higher excitation, the lines broaden as many features become blends of several lines.

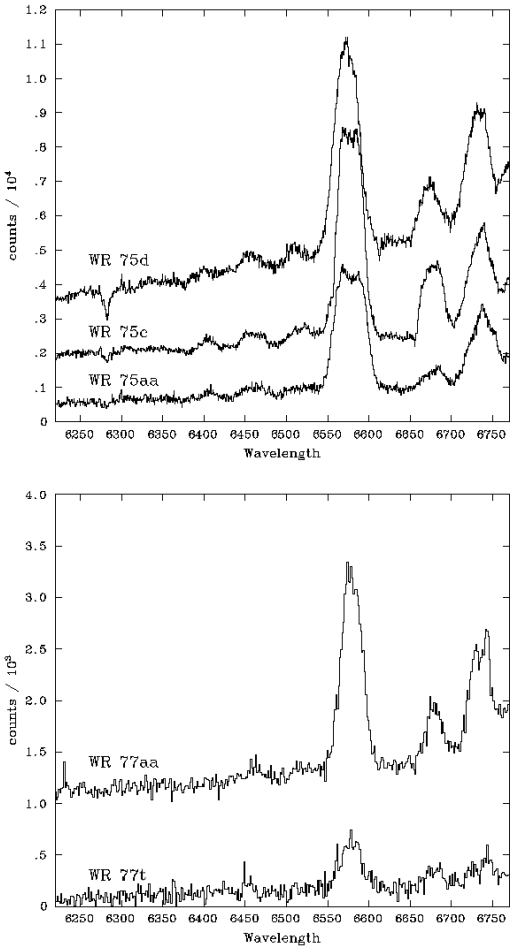

Figure 3. The 6200 - 6800 Å spectra of the 5 new WR stars, offset vertically. Upper: WR 75d, 75c and 75aa. Lower: WR 77aa, 77t. Note the difference in scale between the two panels.

The strongest emission feature seen in the 6dF spectra, the 6570Å blend of He II 6560 Å and C II 6578,82 Å, is a good example of this process: The helium line grows in prominence within the blend (towards earlier spectral types. Examination of figure 4 shows that the shape of the line profile of the ~ 6570 Å feature changes markedly between subtypes WC8 and WC9. In the WC8 spectrum this feature is very obviously a blend, with the C II 6578,6582 Å doublet weaker than the He II 6561 Å emission, but in the WC9 spectrum the blend is dominated by C II, with He II 6560 Å virtually absent. Since the measured central wavelength of the feature in our spectra is 6577.5 Å in four cases and 6573.3 Å in the other (WR 75aa), implying C II dominance, a spectral type of WC9 is implied for all five stars. In support of this assignment, the He II 6405 Å emission in our WR stars is weaker than the adjacent carbon-dominated 6462 Å and 6515 Å emission features, as seen in the WC9 spectrum shown in figure 4.

The Starlink DIPSO package was used to spectrally fit the lines and provide values for equivalent widths (EW) and full widths at half maximum (FWHM). For the weaker line EW determinations and all FWHM measurements, gaussian fitting was used. To prepare for this, continuum fits were derived for each spectrum and then divided. This procedure was hampered by the narrow spectral range: the red end of the observed spectra lies at 6775 Å and, as

Table 3. Log of SHS 6dF follow-up observations conducted from 26th - 30th March 2004.

Field	R Mag range	Observation date	UT Start	Object frame exposures	Sky-offset exposures	Seeing	Other information
HAL0349	12-14	26-03-2004	13:38	6 x 1200	2 x 1200	$\sim 1''$	offset (RA,Dec:-5 -10, +10 +5)
HAL0413	12-14	28-03-2004	13:50	3 x 1200	1 x 1200	$\sim 2''$	offset (RA,Dec:+12 +7)
HAL0413	14-16	29-03-2004	14:50	6 x 1200	3 x 1200	$\sim 2''$	offsets(RA,Dec:+12 -7, -7 +12, +7 +12)
HAL0414	14-16	27-03-2004	15:44	6 x 1000	2 x 1000	$2 - 4''$	offsets(RA,Dec:-12 -7, -7 +12)

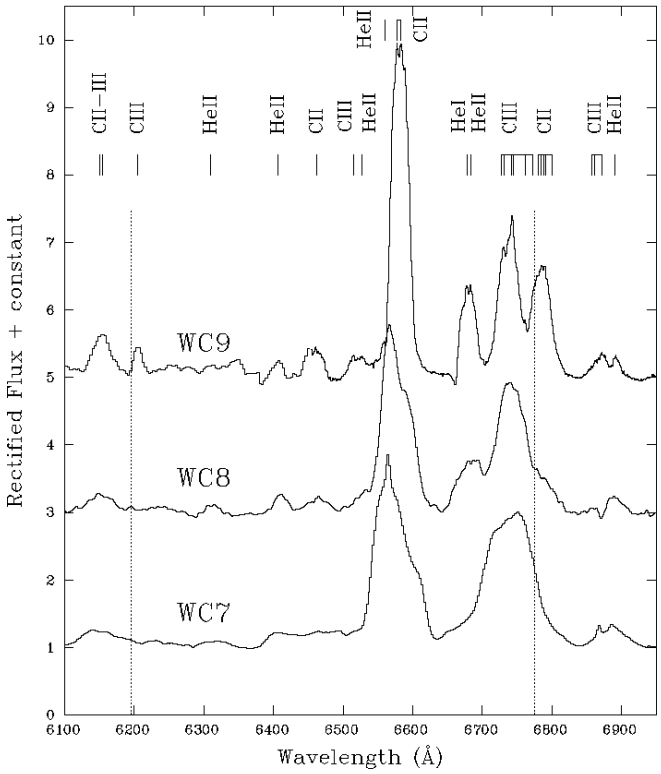

Figure 4. Example 6200 - 7000 Å spectra of late type WC stars. WC7=WR 90, WC8=WR135, WC9=WR103. The vertical dashed lines indicate the limits of our 6dF spectra.

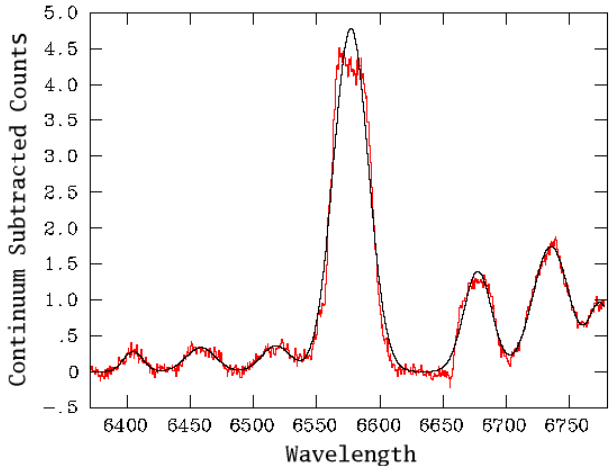

Figure 5. Example spectral line fitting. The 6375-6775 Å spectrum of WR 75c (black), with the gaussian fits overlaid (red).

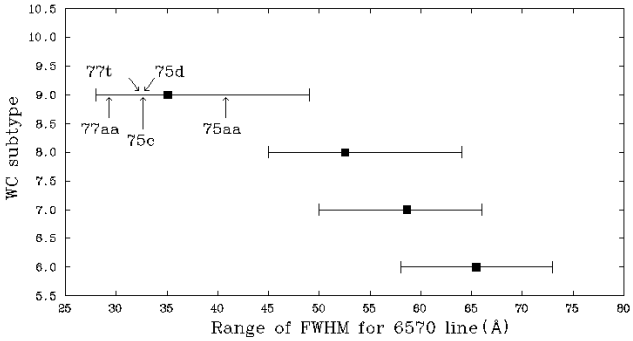

Figure 6. FWHM data for the 6570 Å feature as a function of WC star subtype, taken from Torres-Dodgen & Massey's 1988 spectrophotometric atlas. All of the WC stars of subtype 6, 7, 8, or 9 in this catalogue were used, provided data in the 6500 Å region of their spectra were available. Solid lines indicate the FWHM range spanned, filled squares show the mean FWHM for the subtype while the FWHMs of the new WC9 stars are indicated with arrows. The FWHM were measured via gaussian fitting.

figure 4 shows, this part of the spectrum is crowded with emission lines which make accurate continuum determination difficult. For all objects the continuum was estimated separately for the regions 6195-6650 Å and 6530-6775 Å using a linear fit in both sections. Figure 5 shows an example continuum-subtracted spectral line fit for WR 75c: this demonstrates the need to determine the EW of the 6570 Å and 6680 Å blends by the more direct device of integration of the emission profile counts – simple gaussian fits to these clearly non-gaussian features typically overestimate the line EW. The EWs for the 6570 Å and 6680 Å blends in Table 4 were measured by integrating the net line emission counts after normalising the spectrum locally. It was not possible to fit all the listed emission features for all 5 stars: e.g. for the faintest member of the sample, WR 77t, gaussians were only fitted to three features.

Some support for the classification of these stars as members of the WC9 class comes from applying the same FWHM fitting method to the 6570Å feature in the WR spectra in the spectrophotometric catalogue of Torres-Dodgen and Massey(1988). Figure 6 shows that, the later the spectral subtype of the star, the smaller the FWHM of the 6570Å emission line blend. All five of the WC stars in our sample fall within the FWHM range for these WC9 stars, and outside the range shown by the WC8 stars. WR 75aa is less clear cut: it presents with the largest FWHM, as well as the shortest central wavelength for this blend – both suggesting a leaning toward the earlier spectral type.

Table 4. Identification and measurements of emission lines in the 6195-6775 Å spectra of the new WR stars.

Wavelength (Å)	Transition ID	WR 75aa –EW(Å)	FWHM(Å)	WR 75c –EW(Å)	FWHM(Å)	WR 75d –EW(Å)	FWHM(Å)
6405	He II 15-5	11.2±0.7	26.2±5.2	5.7±0.9	18.7±3.5	5.0±0.5	36.7±4.9
6462	C II $2s^2$6g→$2s^2$4f	20.1±1.9	36.9±4.2	10.4±1.1	28.5±3.4	6.1±0.4	27.8±2.1
6515	C III 2s9h→2s6g He II 14-5	12.4±1.4	26.7±3.0	10.8±1.1	27.3±2.6	3.2±0.2	17.1±1.5
6570	He II 6-4 C II 3p→$2s^2$	169±10	40.8±0.4	158±3	32.6±0.3	74.0±0.8	32.8±0.2
6680	He I 1s3d→1s2p He II 13-5	17.2±5.0	29.5±2.4	38.7±5.0	26.7±0.4	12.8±0.9	26.6±0.6
6735	C II M21,M16.03 C III M3	75.8±2.6	35.9±1.5	74.8±1.1	35.2±0.6	34.7±0.4	33.5±0.4

Wavelength (Å)	Transition ID	WR 77aa –EW(Å)	FWHM(Å)	WR 77t –EW(Å)	FWHM(Å)
6405	He II 15-5				
6462	C II $2s^2$6g→$2s^2$4f	28.0±3.1	41.3±5.6	10.4±2.3	9.8±2.1
6515 ,	C III 2s9h→2s6g He II 14-5	11.3±2.3	27.8±6.2		
6570	He II 6-4 C II 3p→$2s^2$	178±10	29.3±0.4	105±10	32.2±1.6
6680	He I 1s3d→1s2p He II 13-5	32±5	19.0±2.1	32±5	27.4±5.6
6735	C II M21,M16.03 C III M3	53.5±2.7	29.5±1.7		

Whilst the five WC9 stars have very similar spectra, there are some significant differences between them, which are noted below:

Diffuse interstellar band (DIB) absorption is seen in the spectra of both WR 75c and WR 75d. For WR 75d the DIBs at 6284 Å and 6613 Å are both seen, while WR 75c shows evidence of absorption at 6284 Å only. The DIB properties will be relevant to the discussion of reddening in the next section.

Relatively strong emission in the He II 6405 Å line is shown by WR 75c. The strength of this line compared to the carbon lines is a possible indication that this star belongs to the small subgroup of WC9 stars that have never shown evidence of circumstellar dust emission. This view derives from the work of Williams & van der Hucht (2000) in which it is shown that other WC9 stars of this type (WR 81, 88, 92) also possess relatively enhanced He II emission.

Almost the opposite pattern of EW ratios to that observed for WR 75c is seen in the spectrum of WR 77aa. When compared to the other WC9 stars presented here, the HeII contribution to its spectrum is slight: there is no definite detection of HeII 6408, while the 6570 Å blend is somewhat redshifted and narrower compared to the other WC9 stars presented here, suggesting little contribution from HeII 6562.

Lastly we note that binarity is suspected for WR 75d on the basis that the EW of its 6570 Å emission blend is under half that seen in WRs 75aa, 75c and 77aa. This cannot be more than a suspicion since WR emission line EWs show significant differences, object to object, even among apparently single stars (eg. Torres & Conti, 1984).

5 DUST EMISSION, REDDENING AND DISTANCE DETERMINATION

5.1 Reddening estimation

The next step in assessing the physical properties of the 5 new WR stars was to determine the interstellar extinctions towards them and to decide if they display NIR colours indicative of circumstellar dust emission. Of the 30 WC9 stars contained within the Seventh catalogue of Galactic WR stars (van der Hucht, 2001) only 5 are listed as not possessing circumstellar dust. Most of the known WC9 stars (18) are known to display evidence of either persistent or variable dust emission. The remaining 7 in the catalogue are heavily reddened ($A_V \sim$29 mag) stars within 30pc of the Galactic Center, for which it is to difficult reach any conclusion.

To estimate the reddening of our WC9 stars, data from the 2MASS and GSC 2.2 catalogues were obtained for 11 well studied WC9 stars and the five newly discovered objects (Table 5). We split the 11 known WC9 stars into the group of five without NIR excesses and a group of six with excesses. We chose to use the 2MASS JHK and GSC 2.2 R magnitudes to derive measures of the spectral energy distributions (SEDs) of our sample because reasonably uniform data on all 16 WR stars are contained within these catalogues. Table 5 gives the relevant magnitudes.

The initial assumption of our method for determining reddenings is that all WC9 stars have similar unreddened optical/NIR colours, allowing the better known examples to serve as references SEDs for the newly discovered objects. More specifically, we dereddened the magnitudes of the five WC9 stars without NIR dust excesses, in order to obtain their intrinsic colours which were averaged to use as template colours. In the process we noted that WR 92 is somewhat discrepant, but not so much that its inclusion significantly altered the derived SED template. Initially, we considered just red and infrared wavelengths. For these stars we adopt the

Table 5. Magnitudes for a selection of known WC9 stars and for all five newly-discovered WC9 stars. The B_J and I magnitudes are taken from the USNO B1 catalog, the R magnitudes are from the GSC 2.2 catalog, while the JHK magnitudes are 2MASS measurements.We also quote approximate MSX A-band (8.28 μm) magnitudes, $m_{8.28}$, where available. Exceptions are the R mags for WR 103 - taken from the USNO catalog and the I mags of WR 119 and 77t taken from the DENIS catalogue.

WR	B_J	R	I	J	H	K	$m_{8.28}$
Known WC9 Stars without NIR dust excesses							
75a	16.2	14.1±0.4	11.96±0.3	9.96±0.02	9.18±0.03	8.50±0.02	
75b	15.8	14.1±0.4	11.65±0.3	9.76±0.03	9.00±0.03	8.36±0.03	
81	13.2	11.0±0.5	10.18±0.3	8.29±0.02	7.76±0.05	7.12±0.02	5.8
88	14.1	11.6±0.4	10.62±0.3	9.03±0.02	8.56±0.04	8.05±0.04	6.7
92	10.5	10.2±0.1	10.12±0.3	9.50±0.03	9.22±0.03	8.82±0.02	
Known WC9 Stars with NIR dust excesses							
65	14.4	12.3±0.4	10.96±0.3	8.46±0.02	7.28±0.05	6.17±0.03	4.5
73	15.5	13.5±0.3	11.81±0.3	10.32±0.02	8.79±0.05	7.47±0.02	4.8
95	14.5	12.3±1.1	10.92±0.3	8.29±0.02	6.67±0.03	5.27±0.02	2.4
103	8.9	8.7±0.3	8.64±0.3	7.75±0.03	7.21±0.05	6.37±0.03	4.3
104	13.9	12.1±0.4	10.31±0.3	6.67±0.03	4.34±0.24	2.42±0.26	-1.9
119	13.3	11.3±0.4	10.99±0.3	9.50±0.02	8.43±0.06	7.27±0.02	4.8
New WC9 Stars							
75aa	17.5	15.5±0.2	14.35±0.3	12.03±0.02	10.73±0.02	9.46±0.02	6.9
75c	16.4	14.2±0.2	13.11±0.3	11.63±0.02	11.12±0.02	10.52±0.02	
75d	17.0	14.8±0.2	11.99±0.3	10.68±0.02	9.88±0.02	9.12±0.02	
77aa	19.3	16.0±0.2	13.54±0.3	10.04±0.02	8.21±0.02	6.73±0.03	4.0
77t	18.9	16.1±0.5	13.85±0.4	10.65±0.03	9.41±0.02	8.32±0.02	6.0

A_V values from Table 28 of the seventh catalogue of WR stars (van der Hucht, 2001) and used the tabulation of A_λ/A_V of Cardelli, Clayton & Mathis (1989) to derive dereddened magnitudes with a standard Galactic reddening law, corresponding to R=3.1, applied.

To estimate the reddenings towards other stars in our sample, we dereddened their observed NIR magnitudes until the best match to our adopted dereddened NIR colours was achieved. In this process, we attached the highest weight to matching $(J-K)$. However, this method can only give reliable reddening estimates for the minority of WC9 stars without dust emission. When instead, there is significant contamination of the NIR SED by dust emission, this approach results in an anomalously high derived visual extinction. The listed $A_{V,(K)}$ errors in Table 6 take no account of this systematic difficulty. They indicate only the results of propagating through the errors inherent to the photometry.

Overestimation of $A_{V,(K)}$, due to the contamination of, especially, K-band light by warm dust emission, can be put to use as a useful pointer to NIR dust emission. To do this and to test the validity of the $A_{V,(K)}$ values deduced from matching the NIR colours, we used our derived intrinsic WC9 $(R-K)$ colour, first to obtain dereddened R magnitudes from the dereddened K magnitudes for all 16 WC9 stars in the sample, and second, 'predicted' reddened R magnitudes (reddened by amounts consistent with the 2MASS NIR colour fitting). In the absence of NIR dust emission these predicted magnitudes, $R_{(\mathrm{K})}$, should roughly match observed R magnitudes taken from the GSC 2.2 catalogue. For stars with NIR dust emission, this procedure yields clearly discrepant, fainter magnitudes than those observed. Hence, objects with large $(R-R_{(\mathrm{K})})$ are picked out as NIR excess objects. The results of applying this check to our sample are given in Table 6. In this way we successfully reproduce the division of the known WR stars into the NIR-excess and no-excess categories, with the exception of WR 92 and WR 103 which cannot be assigned to either category solely on the basis of their $(R-R_{(\mathrm{K})})$ values. These are 'intermediate' cases where $(R-R_{(\mathrm{K})}) \sim 1$. For the newly discovered WC9 stars, we find that both WR 75c and WR 75d appear to be without NIR dust emission, increasing the number of recognised Galactic 'non-dusty' WC9 stars from 5 to 7. In WR 77t, $(R-R_{(\mathrm{K})})$ is ~ 1 making it intermediate such that we cannot exclude or confirm the presence of a NIR dust excess.

The problem, for extinction estimation, of dust emission contaminating the NIR SEDs of WC9 stars can be overcome by using shorter wavelength magnitudes that are uncontaminated. To this end, the B_J magnitudes of the stars in our sample given in the USNO B1.0 catalogue were collected, and are believed to be accurate to $\pm$ 0.3 magnitudes (Monet et al. 2003). Essentially the same reddening determination method was then applied to all stars in our sample, with the difference that all stars were dereddened to a common intrinsic (B_J-J) value, in place of $(J-K)$. The (B_J-J) colour index was chosen for this purpose because it covers a region of the SED which we would expect to be far less affected by dust emission than (J-K) whilst spanning a wide wavelength range. Since the photographic B_J bandpass is a broad one and these WC9 stars are significantly reddened, we re-used the group of five known WC9 stars without NIR excesses, this time to serve as templates to establish a best estimate for the effective wavelength of the B_J bandpass. We found this to be $\sim$4800 Å, fixing $A_{(B_J)}/A_\lambda$ to be 1.1: these give a mean intrinsic (B_J-J) colour of -0.5 for the catalogue reddenings of these five objects. Resulting estimates of extinctions ($A_{V,(B)}$) calculated on this basis for all the WC9 stars are listed in Table 6. The errors on these estimates are again from propagation of photometric error only.

For the already known WR stars there is now reasonable, if less precise, agreement between our new estimated extinctions,

Table 6. Reddening and distance estimates. The column headed 'dust?' notes whether NIR excesses attributable to dust emission are present. The following columns give derived reddenings and related quantities: $A_{V,(cat)}$ is the visual extinction given in Table 28 of the seventh catalogue of galactic WR stars (van der Hucht, 2001); $A_{V,(K)}$ is the extinction we derive using the 2MASS JHK data; $R - R_{(K)}$ is the difference between the GSC 2.2 R magnitude and the predicted R magnitude based on the NIR-based reddening estimate; $A_{V,(B)}$ is the extinction obtained from the $(B_J - J)$ colour; D_{cat} is the distance also given in Table 28 of the WR catalogue (van der Hucht (2001); D is the estimated distance, and was used in conjunction with the Galactic co-ordinates to estimate R_G, the galactocentric radius. The data in these columns were derived using a reference SED determined from the mean dereddened colours of the 5 non-dusty WC9 stars WR 75a, 75b, 81, 88 and 92, adopting A_V values from van der Hucht(2001).

WR	dust?	$A_{V,cat}$	$A_{V,(K)}$	$R - R_{(K)}$	$A_{V,(B)}$	D_{cat} (kpc)	D (kpc)	R_G (kpc)
Known WC9 stars without NIR dust excesses								
75a	no	8.1	8.6±0.6	-0.1	8.2±0.4	1.6	3.3±0.5	
75b	no	8.9	8.2±0.7	-0.5	7.9±0.4	2.3	3.6±0.6	
81	no	6.4	6.9±0.5	0.5	6.6±0.4	1.6	1.4±0.2	
88	no	6.0	5.8±0.7	0.1	6.7±0.4	2.3	1.7±0.3	
92	no	2.1	4.0±0.6	1.2	1.8±0.4	3.8	5.0±0.8	
Known WC9 stars with NIR dust excesses								
65	yes	7.6	13.4±0.6	2.4	7.8±0.4	3.3	1.6±0.3	
73	yes	6.9	16.6±0.5	4.6	6.9±0.4	3.9	3.8±0.6	
95	yes	7.4	17.6±0.4	4.2	8.2±0.4	2.1	1.4±0.2	
103	yes	1.8	8.1±0.7	1.6	2.0±0.4	2.2	2.3±0.4	
104	yes	7.2	24.7±1.7	6.1	8.7±0.4	2.3	1.1±0.2	
119	yes	4.4	13.1±0.5	4.3	5.3±0.4	3.3	2.5±0.4	
New WC9 stars								
75aa	yes		15.0±0.5	3.6	7.3 ±0.4		8.4±1.3	3.4±0.8
75c	no		6.5±0.5	0.5	6.4 ±0.6		6.2±1.4	3.5±1.7
75d	no		9.1±0.5	0.2	8.3 ±0.4		4.3±0.7	4.8±1.4
77aa	yes		19.3±0.6	3.1	11.9 ±0.4		2.2±0.4	6.5±1.0
77t			13.6±0.6	0.9	10.3 ±0.4		3.9±0.6	4.9±1.5

$A_{V,(B)}$, and the already published catalogue values ($A_{V,(cat)}$): the mean difference is ∼0.5 magnitudes. As a necessary result of the method adopted, the agreement in the mean is best for the known WC9 stars with no apparent dust excess, since these provided the mean template $(B_J - J)$ colours. There is evidence of a positive offset for the known WC9 stars showing NIR dust emission, in the sense that $A_{V,(B)}$ always exceeds $A_{V,cat}$. This excess is most noticeable for WR 104. We attribute this to dust emission being a greater contaminant of the J band flux in this object. Nevertheless it is clear that $A_{V,(B)}$ is a very much better measure of the visual extinction for objects with dust emission than $A_{V,(K)}$.

We conclude that for WR 75c and 75d, without NIR continuum excesses, that $A_{V,(K)} = 6.1 \pm 0.5$ and 8.8 ± 0.5 are to be preferred as extinction estimates. For WR 75aa, 77aa and 77t, in which there is evidence of dust emission, the more approximate estimates exploiting blue photographic magnitudes are to be preferred: namely, $A_{V,(B)} = 7.3 \pm 0.7$, 11.9 ± 0.7 and 10.3 ± 0.7.

5.2 Distance estimates, observed SEDs and other data

The derived extinctions, $A_{V,(B)}$, can be combined with the tabulated GSC 2.2 R magnitudes and the assumption $M_V = M_R = -4.6$ (using the value of M_V from van der Hucht 2001), in order to estimate distances to the newly-discovered WC9 stars. These are given in the penultimate column of Table 6. The errors specified are likely to be optimistic given that the distances calculated for the known WC9 stars differ from their catalogued values by 1–2 kpc – differences larger than the errors deriving from the photometric uncertainties alone. The probable causes of this scatter are the limited reliability of the individual GSC 2.2 R magnitudes and uncertainties in A_V due to possible differences between the assumed and actual reddening law for different objects. In addition, among the known WC9 stars with NIR excesses, there is evidence of a systematic effect such that our estimated distances are always too low. This can be explained by the $A_{V,(B)}$ estimates being typically higher than they are in reality (as we suspect, see above in Section 5.1). We conclude that the distance estimates to the five newly-discovered WC9 stars are rough values only – more reliable CCD photometry can certainly improve the situation. For WRs 75aa, 77aa and 77t there are further grounds to suspect our distance estimates are on the low side.

In figure 7 we plot the optical and NIR colours we have gathered from the literature on the newly discovered objects. It confirms that WR 75c and WR 75d are, in the NIR at least, the most similar in colour to the non-dusty WC9 stars. Because of this and the success with which we are able to 'predict' the GSC 2.2 R magnitude, we are confident we have measured the visual extinctions of WR 75c and WR 75d in a self-consistent way.

We have checked for MSX (Egan & Price 1996) detections of mid infrared (8.28 μm) emission at or near the positions of our sample WC9 stars. This shows the expected correlation between detectable NIR excesses and mid-IR flux: the 3 new WC9 stars deduced to have NIR excesses were detected by MSX, while the two without excesses (WR 75c and 75d) were not. The $m_{8.28}$ magnitudes included in Table 5 are based on a zero magnitude flux from Vega at 8.28 μm of 55 Jy, derived by normalising a Kurucz $T_{\rm eff}$ = 9400 K, log g = 3.90 model to Vega's 5556 Å flux of 3540 Jy. The IR emission of the newly-discovered WC9 stars is fairly faint, which should not be a surprise given that they escaped detection by

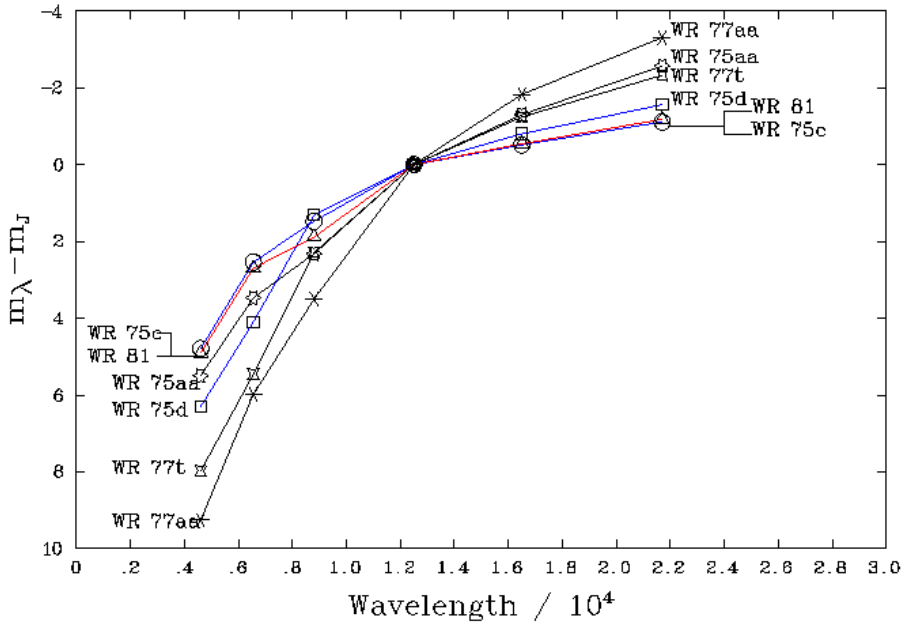

Figure 7. The observed SEDs of the newly discovered WC9 stars. For comparison, the data on the non-dusty star WR 81 are also plotted. The ordinate is the broadband magnitude difference, $m_\lambda - m_J$, and is derived from the data given in table 5, and the I magnitudes given in the USNO B1 catalogue. At NIR wavelengths, WR 75c and WR 75d (shown in blue) are most like WR 81 (shown in red) even before dereddening.

Table 7. Identification and measurement of the observed DIB features. λ_{ref} and $_{ref}$ refer to the properties of HD 183143.

λ_{ref} (Å)	λ_{obs} (Å)	FWHM (Å)	EW$_{ref}$ (mÅ)	EW$_{obj}$ (mÅ)	$A_{V,(DIB)}$
WR 75c:					
6283.86	6282.0	6.2	1945	1600	3.3
WR 75d:					
6283.86	6282.2	8.5	1945	3400	6.9
6613.62	6612.5	2.8	358	500	5.5

previous IR colour-based searches for dusty Wolf-Rayet stars (e.g. Cohen's 1995 IRAS search).

As mentioned in section 4, both of the new WC9 stars lacking NIR dust excesses display DIB absorption features in their spectra. The EWs of these DIBs can be compared to those of HD 183143, the standard DIB reference object (Herbig 1995), in order to obtain a rough lower limit to the interstellar reddening. The EW and FWHM values of the DIB features were measured using the same spectral fitting procedure as was applied to the emission lines, and the results are given in Table 7. The $A_{V,(DIB)}$ values for WR 75c and 75d resulting from such a comparison are considerably lower than those estimated from their NIR colours in Table 6. This suggests that about half of the reddening towards these stars may be associated with molecular gas – not commonly thought to host the DIB carriers – rather than with diffuse-cloud atomic gas that does. (see Herbig 1995 and references therein).

The coordinates of WR 77aa place it within 5 arcmin of Westerlund 1, the star cluster which first motivated our investigation of this region. WR 77aa has the largest reddening ($A_V = 11.9 \pm 0.7$ mags) of the five WC9 stars discussed here, not far short of the A_V = 13.6 estimated by Clark et al. (2005) for a number of OB supergiants at the core of Wd 1, for which Clark et al. estimate a distance of 2 – 5.5 kpc. The distance of 2.2±1.4 kpc derived here for WR 77aa opens the possibility of association with Wd 1.

6 DISCUSSION

The allocation of a WC9 class to all five of the WR stars discussed here is consistent with the already known galactic distribution of this class of object. The 5 WC9 stars presented here fall within $337.0^\circ < \ell < 342^\circ$ and $-0.35^\circ < b < 2.80^\circ$ with galactocentric radii in the range $3.4 \lesssim R_G \lesssim 6.5$ kpc (Table 6). This finding is based on distance estimates that are presently uncertain by as much as ∼2 kpc. Once CCD photometry becomes available for these newly-discovered WC9 stars, these errors will fall.

The small region encompassing the five new Wolf-Rayet stars partially overlaps the area covered by the Shara et al. (1991, 1999) survey for galactic WR stars, with WR 75aa, 75d and 77aa all falling within the overlap region. Their survey used the comparison of narrow and broadband photometry centred on the 4686 Å WR emission line feature to select WR candidates for spectroscopic observation. It probed down to a blue magnitude of ∼19 and was considered to be complete for the detection of single WR stars at the 90% level down to ∼17.5. The broadband magnitudes listed by Shara et al. for the stars discovered by their survey tend to be fainter than the B_J magnitudes for the same stars given in either the whole-sky GSC 2.2 or USNO B1.0 catalogues. This no doubt reflects the difference between effective B mean wavelengths, which are somewhat shorter in the Shara et al measurements. However, as USNO B1.0 magnitudes are also available for the new discoveries

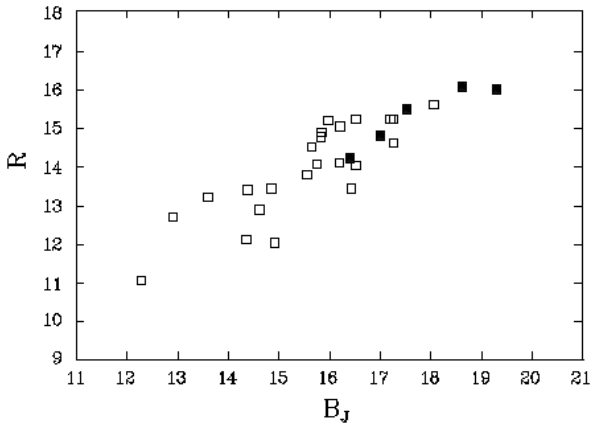

Figure 8. A plot of GSC 2.2 R magnitudes against USNO B_J magnitudes for the WR stars detected by the Shara et al (1999) survey of the southern Galactic Plane (open squares) and the newly discovered WC9 stars presented in this paper (filled squares). Only 27 of the 35 WR stars detected by Shara et al. are plotted, as not all stars in their sample had reliable data available from both the GSC 2.2 and USNO catalogues.

we need to use them in comparing the B_J and R magnitudes of the new WC9 stars with those of the Shara et al sample (Fig 8). This comparison demonstrates that the new Wolf-Rayet stars selected from the SHS, with R magnitudes in the range $14 < R < 16$, overlap with and reach beyond the faint end of the Shara et al survey.

The Shara et al (1991) survey was the last large scale optical survey for galactic WR stars. All other galactic WR star discoveries since 1991 have either been the result of the reclassification of previously known emission line objects or resulted from NIR/MIR/radio observations. Longer wavelengths suffer far less severely from the effects of extinction, and so allow the detection of WR stars in distant parts of the galaxy obscured by large columns of dust. Recent WR star searches have therefore focused on K band (2μm) observations. In such searches there is a potential bias toward the discovery of WC9 stars with NIR continuum excesses as they are brighter at NIR wavelengths. But, at the same time emission line EWs in WC9 stars NIR spectra may be reduced by the added dust continuum, and therefore become harder to detect.

In order to estimate the frequency of occurrence of dust emission in late WC stars, a sample that is flux-limited at wavelengths shortward of 1 μm could help avoid the biases that might be acting at longer wavelengths. Of the five newly-discovered WC9 stars presented here, selected via their strong C II $\lambda\lambda$6578,6582 emission, two have turned out not to possess NIR excesses attributable to dust. Up to now, just five – out of the more than 30 known WC9 stars – have been recognised as belonging to this category. Three of them were discussed by Williams & van der Hucht (2000). The other two, WR 75a and 75b, were products of the Shara et al survey, and were recognised as lacking NIR excesses by van der Hucht (2001). So all seven objects, making up this group, are optical discoveries.

It was noted a long time ago (e.g. Smith 1968) that Galactic WC9 stars are found only inside the Solar Circle. Despite the large increase in the numbers of known Galactic WC9 stars since then, this conclusion still holds. In the lower metallicity Large Magellanic and Small Magellanic Clouds, no WC9 stars at all are known[1] AT99-4 is listed as type WC9+O8V in the Breysacher et al (1999) catalogue of WR stars in the LMC, but it is noted that this typing had been dismissed by Moffat (1991). Heydari-Malayeri & Melnick (1992) confirmed that the older WC9 assignment was not warranted. . In contrast to this, M83 – a metal rich spiral like the Milky Way – has been shown to host a large number of late WC stars, including some WC9s (Hadfield et al, 2005). Another aspect to this is the recognition that there is a gradient in the number of WC type stars relative to WN stars such that the WC types are relatively more numerous at smaller galactocentric distances (R_G, Massey & Johnson 1998). Our selection should not be biased towards the selection of WC9 stars as all WR subclasses show Hα , HeII or C emission which falls within our 70Å bandpass (cf. discovery of WO star WR 93b, Drew et al 2004). All 5 sharing the same WR subtype can therefore be seen as an indication of the preponderance of late WC stars in the inner Milky Way.

However the fact remains that extrapolation inwards of the Solar Circle of the trend in the surface density of *all* types of WR star would indicate many more WR stars at $R_G < R_\odot$ might well be present than are actually known (see figure 10 in van der Hucht 2001)! Accordingly, it is interesting and encouraging that this relatively shallow trawl of 4 SHS fields, based on red rather than either infrared or short wavelength optical data, has already produced 5 new strongly-reddened WR stars scattered across a mere $\sim$8 square degrees, albeit embedded within a total search area of $\sim$48 square degrees. No two of the stars found are likely to be within the same cluster. We conclude that optical searches of the Galactic Plane for new massive WR stars remain worthwhile, if taken to greater depths of $R \sim 19$ that still lie well within the grasp of even 4-metre class telescopes.

Acknowledgements EH and MP both acknowledge the support of postgraduate studentships funded by the Particle Physics & Astronomy Research Council of the United Kingdom. This paper makes use of: data obtained with the AAO/UK Schmidt Telescope at Siding Spring Observatory, NSW, Australia; the SIMBAD database, operated at CDS, Strasbourg, France; data products from the Two Micron All Sky Survey; data from the USNOFS Image and Catalogue archive; data from the Guide Star Catalogue II and data from the DEep Near Infrared Survey (DENIS). We also acknowledge the use of Starlink software in both the reduction and analysis of our spectroscopic data.

REFERENCES

Breysacher J., Azzopardi M., Testor, G., 1999, A&AS, 137, 117
Cardelli J.A., Clayton G.C., Mathis J.S. 1989, ApJ, 345, 245
Clark J.S., Negueruela I. 2002, A&A, 396, L25
Clark J. S., Negueruela I., Crowther P. A., Goodwin S. P. 2005, A&A, 434, 949
Cohen M. 1995, ApJS, 100, 413
Drew J.E., et al. 2004, MNRAS, 351, 206
Egan M.P., Price S.D. 1996, AJ, 112, 2862
Herbig G.H. 1995, ARA&A, 33, 19
Hillier D. J., 2003, in *A Massive Star Odyssey: From Main Sequence to Supernova*, proc. IAU Sym. No. 212, eds K. van der Hucht, A. Herrero & C. Esteban, Astronomical Society of the Pacific, San Francisco, p.70
Hadfield L.J., Crowther P.A., Schild H., Schmutz., 2005, A&A, in press
Heydari-Malayeri M., Melnick J., 1992, A&A, 258L, 13

[1] B

Homeier N.L., Blum R. D., Pasquali A., Conti P. S., Damineli A. 2003, A&A, 408, 153
LaVine J.L., Eikenberry S., Davis J. 2003, AAS, 203, 1412L
Maeder A., Meynet G., 2000, ARA&A, 38, 143
Massey P., Johnson O., 1998, ApJ, 505, 793
Moffat, A.F.J., 1991, A&A, 244, 9
Monet D.G., et al. 2003, AJ, 125, 984
Negueruela I., Clark J. S., 2005, A&A, in press
Parker Q. A., et al., 2005, MNRAS, submitted
Schlegel D.J., Finkbeiner D.P., Davis M. 1998, ApJ, 500, 525
Schwartz R.D., Persson S.E., Hamann F.W. 1990, AJ, 100, 793
Shara M.M., et al. 1991, AJ, 102, 2
Shara M.M., et al. 1999, AJ, 118, 390
Torres A.V., Conti P.S., 1984, ApJ, 280, 181
Torres-Dodgen A.V., Massey P. 1988, AJ, 96, 3
van der Hucht K. A., 2001, NewAR, 45, 135
Westerlund B.E. 1987, A&AS, 70, 311
Williams P.M., van der Hucht K.A. 2000, MNRAS, 314, 23
Woosley S. E., Heger A., Weaver T. A., 2002, RevMP, 74, 1015